Proceeding of International Joint Conference on UNESA
Homepage : https://proceeding.unesa.ac.id/index.php/pijcu
e-ISSN : 3032-3762

PIJCU, Vol. 3, No. 1, December 2025
Page 1-12

Solar Panel System for an Automatic Bird Pest Repellent (Scarecrow) Driven by a DC Motor

Ajudan Laksamana Yustiarno Putra[1*], Ayusta Lukita Wardani[2*] , Mahendra Widyartono[3] , Aditya Chandra Hermawan[4]
[1*,2,3,4] State University of Surabaya, Surabaya, Indonesia
Corresponding author: ayustawardani@unesa.ac.id

Keywords:
Solar Panel
Scarecrow
DC Motor
LoRa
Bird Pest

ABSTRACT

Bird pests, especially sparrows, are a major problem for rice farmers as they frequently attack crops nearing harvest. This study aims to design and develop an automatic bird repellent device that utilizes movement and sound generated by a scarecrow driven by a DC motor, with solar panels serving as the primary power source. The system consists of two main components: a control system (Tx) and an execution unit (Rx), connected via a LoRa communication module. A 150Wp monocrystalline solar panel is used to supply power and charge a 100Ah LiFePO4 battery as backup. The scarecrow operates in a 22-minute active and 8-minute idle cycle, generating noise using cans filled with stones, designed to mimic a piston mechanism. Test results show the solar panel can produce an average power of 90.06 watts under clear conditions and 64.42 watts during cloudy weather. The scarecrow has an effective reach of up to 45 meters, covering an area of approximately 405 m². This system has proven effective in repelling birds and offers a cost-efficient, environmentally friendly solution to reduce farmers' reliance on conventional methods and improve crop yields.

INTRODUCTION

Rice is a staple food for nearly half of the world's population, particularly in developing countries such as Indonesia. Despite the government's ongoing efforts to enhance rice productivity, farmers still face significant challenges from agricultural pests. These pests can damage various parts of the rice plant—including the roots, stems, leaves, and grains—ultimately reducing harvest yields. Disruptions in agricultural production stability can have far-reaching effects on both the economy and broader aspects of social life. Therefore, effective pest control is essential in ensuring food security and sustaining agricultural productivity (Utami Putri, 2022). Among the most persistent threats to rice crops are birds, particularly sparrows, which often attack in flocks during the pre-harvest period. These birds consume a considerable amount of rice, leading to substantial economic losses for farmers. While some technological solutions—such as ultrasonic repellent systems, servo motor-based devices, and IoT-enabled monitoring—have been developed, many farmers continue to rely on conventional methods such as pesticides or hiring manual labor to guard their fields. Previous studies have explored the use of LoRa-based ultrasonic devices to deter birds using frequencies ranging from 30 kHz to 40 kHz. However, these systems often suffer from limitations in energy efficiency and effective coverage area (Amirul Haq Al Rasyid, 2024). To address these shortcomings, the present study introduces a bird repellent system powered by a 150 Wp monocrystalline solar panel and driven by a 12V DC motor. The system replaces ultrasonic output with physical movement and noise generated by a scarecrow, offering a more sustainable, autonomous, and environmentally friendly alternative for pest management in rice fields.

RESEARCH METHOD

This section outlines several key stages of the study, including the development of research and operational flowcharts, the design of hardware components, selection of materials, and the configuration of the system's wiring layout.

Research Steps

This study involves several stages in designing the research, starting from literature review to data collection, as illustrated in the flowchart shown in Figure 1.

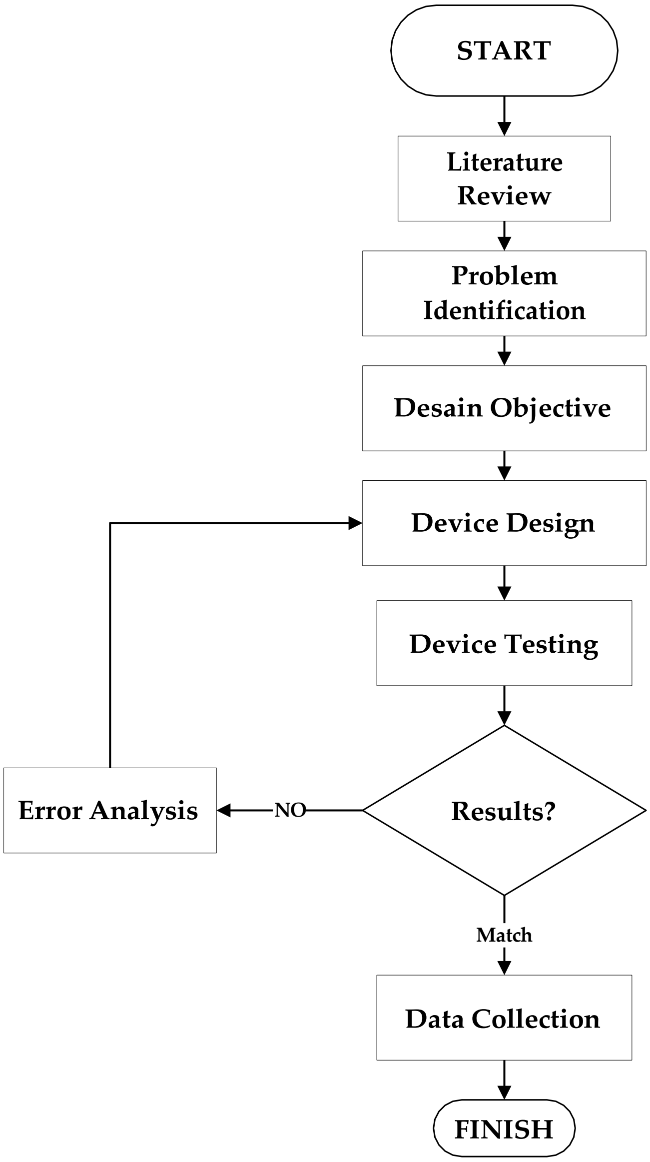

Figure 1. Research Flow Chart
Source : Personal Documents

The following is an explanation of the research diagram as follows:
1. Conduct a review of relevant journals and scientific articles.
2. Identify the core problems that the project aims to solve.
3. Set the design goals and expected outcomes.
4. Design the hardware and (if needed) software components.
5. Test the functionality and performance of the device.
6. Are the test results as expected?
   If No: proceed to Error Analysis, then return to Device Design to revise.
   If Match: continue to Data Collection.
7. Gather and record data based on the working system.

Schematic Diagram of the Tool Design

At this stage, the configuration and functional flow of each system component are determined. The schematic diagram shown in Figure 2 presents the planned arrangement of the components within the tool system.

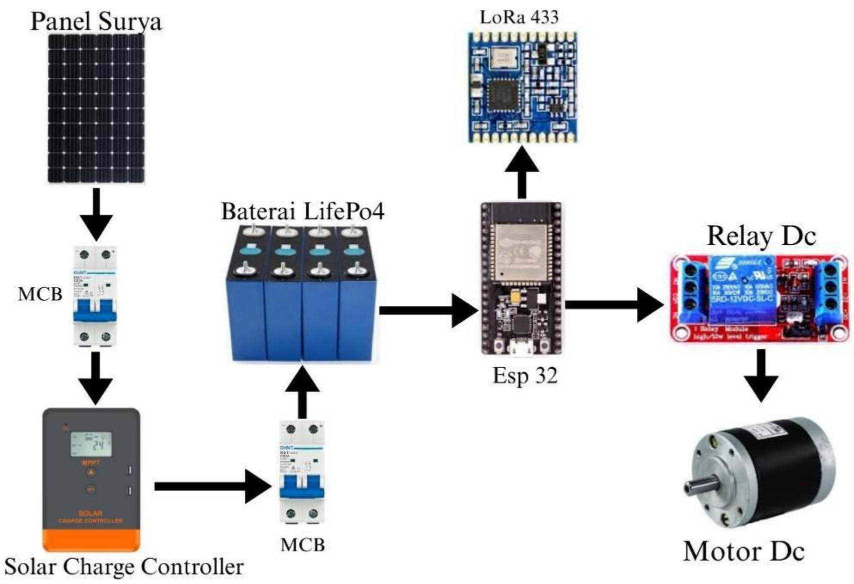

Figure 2. Tool Planning Scheme
Source : Personal Documents

In this system, a solar panel serves as the primary power source. The electricity generated is passed through an MCB (Miniature Circuit Breaker) for safety, and then regulated by a solar charge controller to ensure efficient battery charging. The energy is stored in a LifePo4 battery, which supplies power to the ESP32 microcontroller.
The ESP32 functions as the central controller, connected to a DC relay module that controls a DC motor. Additionally, the ESP32 communicates with a LoRa 433 module for wireless data transmission. The DC motor operation is triggered via the relay based on programmed instructions from the ESP32. This design ensures autonomous operation using renewable energy, with real-time control and wireless communication capabilities.

Working Principle of the Tool

The automatic bird repellent system utilizes a solar-powered energy source as its main power input. Solar radiation is absorbed and converted into DC electricity through a Solar Charge Controller (SCC). A portion of the generated power is used to directly operate a 12V DC motor, while the remaining power is stored in a 12V 100Ah battery to ensure operation during low solar intensity conditions. In the field implementation, particularly in rice paddies, the system is configured to operate from 06:00 AM—coinciding with the time birds begin to target maturing rice fields—until 02:00 PM, when bird activity typically decreases.

The repelling mechanism consists of a scarecrow made from metal cans filled with stones, which are tied together in a linear arrangement and mounted on a pole planted in the field. One end of the pole is fixed to a ground stake, and the other is connected to the DC motor. When the system is activated, the motor moves back and forth, causing the cans to shake and produce a loud rattling noise to deter birds. This movement cycle is programmed to run every 22 minutes with an 8-minute pause interval.

Microcontroller Design Schematic

The design schematic of the microcontroller system is divided into two main modules: the main control unit placed in the field, and the control interface module used for mode selection and system monitoring. Both modules are interconnected using LoRa communication to enable long-distance data transmission.

A. Rx main device

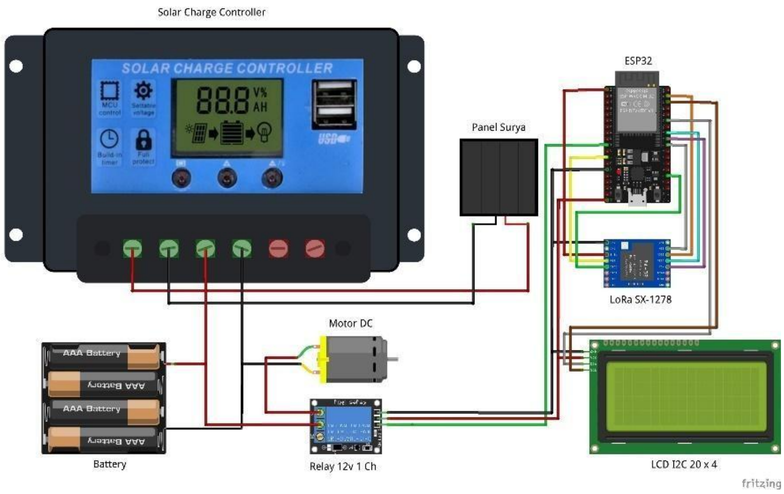

Figure 3. Rx Device Wiring Diagram
Source : Personal Documents

The field module, as illustrated in Figure 3, consists of a solar power supply system and a microcontroller circuit. The solar panel serves as the main energy source and is connected to a Solar Charge Controller (SCC), which regulates the charging process of a 12V 100Ah battery. The battery stores energy and supplies power to a 12V DC motor through a 12V 1-channel relay module, which is controlled by an ESP32 microcontroller. The ESP32 is also connected to a LoRa SX-1278 module for wireless communication and an I2C LCD 20x4 display module for local monitoring. This module controls the movement of a scarecrow made from cans filled with stones, which moves at intervals to generate sound and deter birds. The motor is activated and deactivated based on programmed time intervals (22 minutes ON, 8 minutes OFF) within the operating hours of 06:00 to 14:00.

B. Tx Control Device

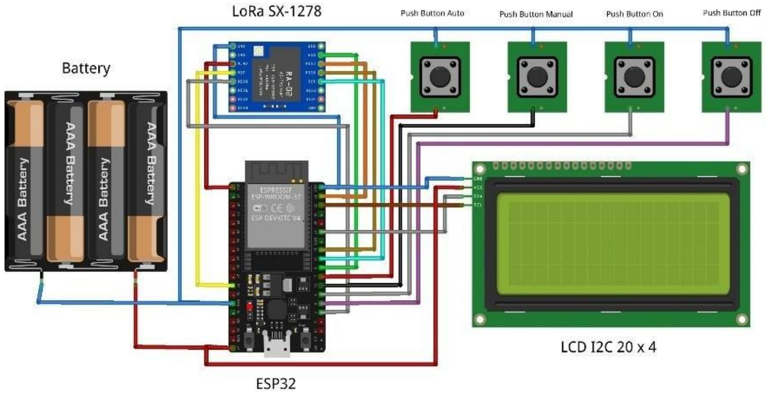

Figure 4. Tx Device Wiring Diagram
Source : Personal Documents

Figure 4 shows the schematic of the control interface module, which includes an ESP32 microcontroller connected to an LCD I2C 20x4, a LoRa SX-1278 module, and four push buttons for manual control. The push buttons include:

- Auto Mode
- Manual Mode
- ON Command
- OFF Command

These buttons allow the user to select the operation mode and send specific commands to the field module. The communication between the modules is carried out via LoRa SX-1278, ensuring low-power, long-range wireless data exchange.

The entire system is powered by a 5V battery pack, providing portability and flexibility in system placement.

RESULTS AND DISCUSSION

The developed scarecrow system is powered by a 150 Wp solar panel and utilizes a 12V 120W DC motor to drive its mechanical movement. To ensure continuous operation under low sunlight conditions, a backup battery is integrated. The system is controlled using an ESP32 microcontroller and a 433 MHz LoRa module, allowing point-to-point communication without internet access, which is suitable for remote rice fields. The system consists of two main units: the Transmitter (Tx) and Receiver (Rx). The Tx unit includes the ESP32 and LoRa module to send control commands (manual/automatic, on/off). The Rx unit, located at the device, receives these commands and executes them through a relay, which controls power to the 12V motor. The Rx is powered by the solar panel and battery via a Solar Charge Controller (SCC).After assembling all components, data collection and functional analysis were carried out to evaluate the system's sensitivity and reliability. The results confirm that the system operates as intended, responding correctly to control inputs and functioning autonomously under field conditions.

Tool Design Results

Figure 5 presents the initial design and the actual realization of the device, which consists of four main components. At the top, a 150 Wp solar panel is mounted with a dedicated support frame. Below it is a panel box that houses the microcontroller, a LiFePO4 battery, and a solar charge controller (SCC). Further down, a 12V DC motor is installed, complete with a mechanical system that drives the scarecrow. Finally, at the bottom, pointed support legs are used to secure the device into the ground, ensuring structural stability and preventing it from toppling over.

Figure 5. Overall view of the Rx (Receiver) device
Source : Personal Documents

Figure 6 shows the control device, referred to as the Tx unit, which consists of three main components: an ESP32, a 433 MHz LoRa module, and a battery as the power source. This device functions to control the main system remotely without requiring an internet connection.

Figure 6. Overall view of the Tx (Receiver) device
Source : Personal Documents

Measuring the Amount of Power Generated by Solar Panels

This test aims to calculate the amount of power (watts) that can be generated by solar panels during the test period, depending on solar irradiation. This will determine how long the device will remain active if powered by solar panels. To obtain current data (Isc), a short circuit must be created by connecting the positive terminal of the panel to the negative terminal of the multimeter and the negative terminal of the panel to the positive terminal of the multimeter. This test is conducted without any load connected to the solar panel.

Table 1. Testing the power generated by solar panels.

Number	Testing Time	Iradiasi (W/m)	Solar Panel Voltage (V)	Solar Panel Current (A)	Power Generated (Watt)
1	06.00	179,4	21,4	1,79	38,306
2	07.00	206,6	21,3	2,07	44,091
3	08.00	276,7	21,3	2,41	51,333
4	09.00	392,7	21,2	3,16	66,992
5	10.00	533,5	21,1	5,35	112,885
6	11.00	822,4	20,9	7,63	113,487
7	12.00	852,1	20,9	7,88	159,467
8	13.00	552,3	21,1	5,43	166,268
9	14.00	239,4	21,3	2,71	57,723
Average power generated					90,06133333

Based on the solar panel testing data table above, it can be concluded that the power generated by solar panels is greatly influenced by the intensity of solar radiation and the current produced. It can be seen that from 6:00 AM to 12:00 PM, solar irradiance increases significantly from 179.4 W/m^2 to a peak of 852.1 W/m^2, followed by an increase in panel current from 1.79 A to 7.88 A. This causes the electrical power generated to also increase, reaching a peak of 159.467 Watts at 12:00. After 12:00 PM, although the irradiance decreased to 239.4 W/m^2 at 2:00 PM, the panel still generated a significant amount of power because the voltage remained relatively stable at around 21V. The average power generated over the entire testing period was 90.06 Watts, indicating that the panel performed quite optimally, especially when sunlight intensity was high.

Measurement of the Range of the Dynamo-Driven Scarecrow

This test aims to measure how far the scarecrow can be moved by a DC motor. It also aims to determine how far commands can be sent by LoRa 433Mhz from the Tx (Transmitter) to the Rx (Receiver) so that the device can be turned on. The measurements are taken in stages every 5 meters, with the coverage area increasing by 45m^2 each time, based on the width of the field (9m x 5m) as it moves backward.

Table 2. Scarecrow range testing

Number	Testing Experiment	Distance from Tx to RX (Meter)	Scarecrow Movement Distance (Meter)	Number of Birds	Displaced or Not	Scope of Coverage Movement (m^2)
1	First	5	5	3	Yes	45
2	Second	10	10	6	Yes	90
3	Third	15	15	2	Yes	135
4	Fourth	20	20	4	Yes	180
5	Fifth	25	25	6	Yes	225
6	Sixth	30	30	0	No	270
7	Seventh	35	35	5	Yes	315
8	Eighth	40	40	12	Yes	360
9	Ninth	45	45	7	Yes	405
10	Tenth	50	50	5	No	450

From the test results in Table 2, it can be seen that from a distance of 5 meters to 50 meters, there were birds that landed and then flew away when the device was turned on to activate the scarecrow. However, at a distance of 30 meters, no birds were found to have landed. The maximum coverage area that the scarecrow can reach and move is 405 square meters, which is 45 square meters short of the problem limit. At a range of 50 meters, the scarecrow moves but does not produce sound, so the birds are not scared away. Similarly, the TX and RX commands transmitted cannot be received properly.

Testing Battery Capacity Degradation Under Load Conditions

This test aims to determine the battery capacity reduction when connected to a DC motor, where the battery functions as a backup. In this test, the solar panel is also connected directly to the load and battery. After testing from start to finish, the battery capacity reduction can be determined every hour. Battery consumption every hour can also be determined.

Table 3. Battery capacity degradation testing

Number	Testing Time	Power Generated by Solar Panels (Watt)	Battery Capacity (Ah)	Battery Depreciation (Ah)
1	06.00-07.00	46,0712	100	5,24
2	07.00-08.00	61,0812	94,76	4,27
3	08.00-09.00	77,7357	90,49	3,06
4	09.00-10.00	73,7234	87,43	3,35
5	10.00-11.00	103,4042	84,08	1,2
6	11.00-12.00	121,9671	82,88	0
7	12.00-13.00	108,7218	83,01	0,81
8	13.00-14.00	104,6837	82,19	1,11
9	14.00-15.00	97,119	81,08	1,66

From the results of the first test in Table 3, it can be seen that on the first day of testing, the battery drained by 20 Ah. Although it was not raining, the power generated by the solar panels could not supply the maximum amount every hour. Therefore, the battery drained every hour, but from 11 a.m. to 12 p.m., there was no drainage because the power generated by the solar panels was sufficient to meet the load requirements. Nevertheless, a backup battery is necessary at certain times, especially during unpredictable seasons. Occasional cloud cover can affect the power generated by the solar panels. However, the power used by the motor can adjust to the supply from the solar panels, but the resulting movement is less than optimal.

Power Testing Graph Obtained from the Panel

Figure 7 shows that current is the parameter most affected by solar irradiance intensity, while voltage tends to remain constant, experiencing only a slight decrease during high current loads. Solar panel performance is most optimal between 10:00 AM and 12:00 PM, when the current generated is sufficiently high to produce maximum power to meet load requirements. Overall, this graph illustrates the characteristic behavior of solar panels, where current production increases at maximum solar irradiance intensity, and voltage is maintained at a stable level for maximum power efficiency. Therefore, a battery is still required when the current generated by the solar panels is insufficient to supply power to the DC motor load.

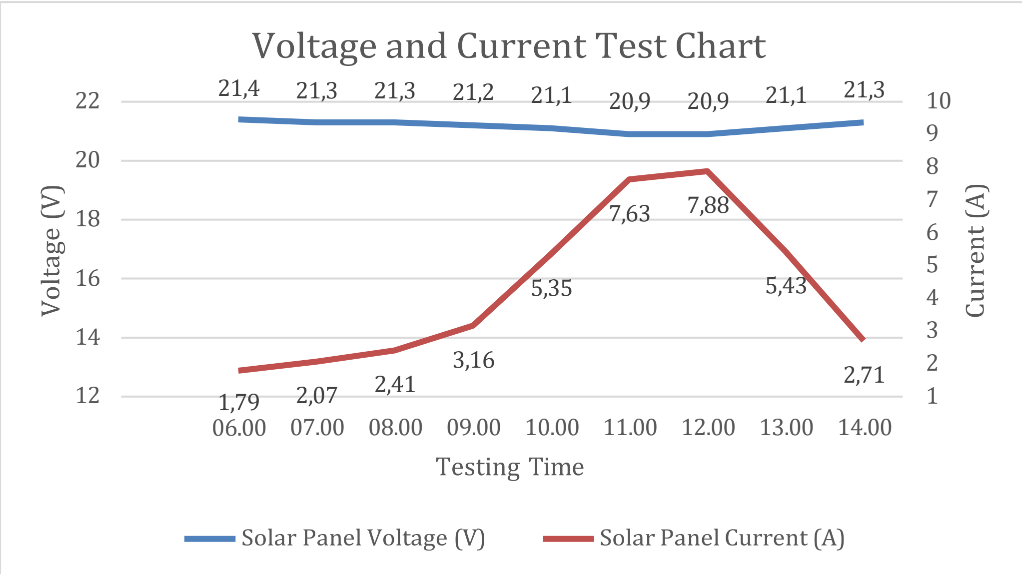

Figure 7. Voltage and Current Test Graph Obtained from the Panel
Source : Personal Documents

Discussion of Battery Capacity Decline Graphs under Load

This discussion focuses on the remaining battery capacity when charged by a solar panel while being used as a backup power source when the solar panel's power is insufficient. The average power consumption during sunny weather is 2.3 Ah. The remaining battery capacity at the end of the test was 81.08 Ah, with a depletion of 18.92 Ah. In the first graph, it was observed that little power was used because the solar panel supplied power sufficiently to the load, which also affects the charging time until the battery is fully charged again.

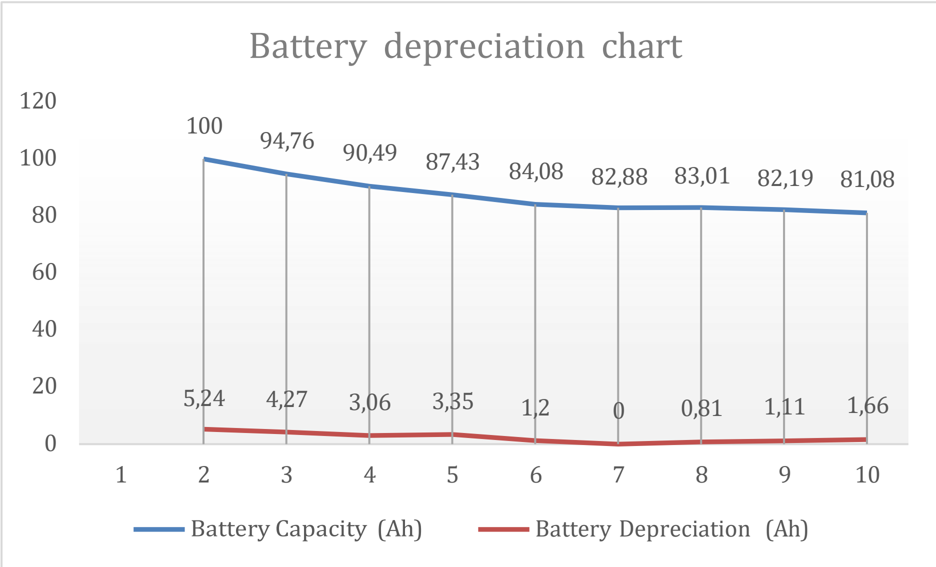

Figure 8. Battery depreciation chart
Source : Personal Documents

CONCLUSION

Based on the results of research on the design of a solar panel system for an automatic bird repellent device (scarecrow) with a DC motor, several conclusions can be drawn, namely:

1. From the results of testing the power generated by the solar panel. It was found that a 150Wp monocrystalline solar panel produces a voltage of 21.5V and a current of 8.29A, generating an average power of 90.06 Watts under clear, slightly cloudy weather conditions. This is sufficient to supply the DC motor's power requirements, although in the morning, additional power supply from the battery is needed. However, under cloudy conditions with a tendency to drizzle, the average power output is 64.42 Watts, with the battery supplying more power.
2. From the results of testing the range of the scarecrow on a test area of 450m^2, it was found that the DC motor can move the scarecrow maximally over an area of 405m^2. Similarly, the range of the 433 MHz LoRa device can transmit commands up to 45 meters. However, at a distance of 50 meters, the scarecrow does not operate at maximum efficiency, nor does the range of the Tx to Rx device. For bird pests, many are deterred even before the birds land, as the device is capable of preventing birds from landing.
3. From the test results, the battery capacity depletion when powered by a solar panel under loaded conditions shows that on a sunny day, the battery consumes an average of 2.3 Ah, leaving a remaining capacity of 81.08 Ah, resulting in a depletion of 18.92 Ah. However, under cloudy conditions, occasional rain, or very

low light, the average battery power consumption is 4.69 Ah, with a depletion of 39.33 Ah. This data was tested on a LiFePo4 battery.

REFERENCES

Abadi, A., Widya, R., & Julsam, J. (2021). Rancang Bangun Pemutus Tegangan Pada Kwh Meter Pelanggan Pln. *Jurnal Andalas: Rekayasa Dan Penerapan Teknologi*, *1*(1), 37–46.

Amirul Haq Al Rasyid, A. L. W. (2024). Rancang Bangun Sistem Pengusir Hama Burung pada Tanaman Padi. *ELPOSYS: Jurnal Sistem Kelistrikan*, *11*(3).

Anggara Trisna Nugraha, Edy Prasetyo Hidayat, Purwidi Asri, Briyen Rangga Prayoga W, & Diego Ilham Yoga Agna. (2023). Prototipe Sistem Pengendalian Dan Pemantauan Cargo Hold Bilge Kapal Dengan Metode Decision Tree Berbasis Mikrokontroler. *Jurnal 7 Samudra*, *8*(2), 93–108.

Hartanto, S. (2022). Tegangan Motor DC Terhadap Berat Barang Pada Ban Berjalan. *Jurnal Elektro*, *10*(2), 174–181.

Hidayatullah, D., & Sulistiyanto, S. (2022). Perancang Alat Pengusir Hama Burung Pipit Pada Tanaman Padi Menggunakan Gelombang Kejut Otomatis Berbasis Internet of Things (IoT). *JEECOM Journal of Electrical Engineering and Computer*, *4*(2), 74–78.

Ismailov, A. S., & Jo'rayev, Z. B. (2022). Study of arduino microcontroller board. *"Science and Education" Scientific Journal*, *3*(3), 172–179. www.openscience.uz

Muhammad Ainun Najib, Sulartopo Sulartopo, Dani Sasmoko, Danang Danang, & Iman Saufik Suasana. (2024). Sistem Pendeteksi Bencana Kebakaran Menggunakan ESP32 Dan Arduino Berbasis WEB. *Neptunus: Jurnal Ilmu Komputer Dan Teknologi Informasi*, *2*(1), 15–24.

Nugraha, R., Fajar, A. M., Adriani, & Rahmania. (2023). Perancangan Sistem Pengaman Rumah Bebasis Microcontroller Dengan Media Telegram. *Vertex Elektro : Jurnal Teknik Elektro UNISMUH*, *15*(1), 26–31.

Radouan Ait Mouha, R. A. (2021). Internet of Things (IoT). *Journal of Data Analysis and Information Processing*, *09*(02), 77–101.

Satyanarayana, P., Sriramdas, N., Madhavi, B., Arun, M., Phani Sai Kumar, N. V., & Gokula Krishnan, V. (2023). Enhancement of Security in IoT Using Modified AES Algorithm for IoT Applications. *International Conference on Sustainable Communication Networks and Application, ICSCNA 2023 - Proceedings*, *March*, 380–386.

Selay, A., Andgha, G. D., Alfarizi, M. A., Bintang, M. I., Falah, M. N., Khaira, M., & Encep, M. (2022). Karimah Tauhid, Volume 1 Nomor 6 (2022), e-ISSN 2963-590X. *Karimah Tauhid*, *1*(2963-590X), 861–862.

Solar, D., Controller, C., Fppt, M., Pelacakan, A., Daya, P., Untuk, P., Pv, P., & Power, D. A. N. (2024). *Vol 10, No. 1, Juli 2024*. *10*(1), 136–145.

Ugwuanyi, S., Paul, G., & Irvine, J. (2021). Survey of iot for developing countries: Performance analysis of lorawan and cellular nb-iot networks. *Electronics (Switzerland)*, *10*(18).

Utami Putri, N. (2022). Rancang Bangun Perangkap Hama Serangga Pada Padi Dengan Sumber Sel Surya (Studi Kasus: Rama Otama 1, Seputih Raman, Lampung Tengah, Lampung). *Electrician*, *16*(1), 123–128.

Wardani, A. L., Andriawan, A. H., & Basyarach, N. A. (2019). Perbandingan Antara Solar Cell Tipe Monocrystaline Dan Polycrystaline Pada Keadaan Terhalang Untuk Pertimbangan Pemilihan Pembangkit Tenaga Surya. *Prosiding Nasional Rekayasa Teknologi Industri Dan Informasi XIV Tahun 2019 (ReTII)*, *2019*(November), 251–256.